

AperTO - Archivio Istituzionale Open Access dell'Università di Torino

**Effects of antebrachial torsion on the measurement of angulation in the frontal plane: A cadaveric radiographic analysis**

**This is the author's manuscript**

*Original Citation:*

*Availability:*

This version is available <http://hdl.handle.net/2318/114922> since 2016-11-25T14:46:23Z

*Published version:*

DOI:10.3415/vcot-10-09-0135

*Terms of use:*

Open Access

Anyone can freely access the full text of works made available as "Open Access". Works made available under a Creative Commons license can be used according to the terms and conditions of said license. Use of all other works requires consent of the right holder (author or publisher) if not exempted from copyright protection by the applicable law.

(Article begins on next page)



UNIVERSITÀ DEGLI STUDI DI TORINO

This is an author version of the contribution published on:

Piras LA, Peirone B, Fox D  
Effects of antebrachial torsion on the measurement of angulation in the frontal  
plane: A cadaveric radiographic analysis  
VETERINARY AND COMPARATIVE ORTHOPAEDICS AND  
TRAUMATOLOGY (2012) 27

# Effects of antebrachial torsion on the measurement of angulation in the frontal plane: A cadaveric radiographic analysis

L. A. Piras<sup>1</sup>; B. Peirone<sup>1</sup>; D. Fox<sup>2</sup>

<sup>1</sup>University of Turin, Animal Pathology, Grugliasco, Italy; <sup>2</sup>University of Missouri, Department of Veterinary Medicine and Surgery, Columbia, Missouri, USA

## Keywords

Angular limb deformity, radioulnar torsion

## Summary

**Objectives:** To quantify the effect of antebrachial torsion on the miscalculation of radial valgus measured radiographically and to assess a radiographic positioning method used to mitigate torsion-associated artifactual miscalculation of concurrent frontal plane angulation.

**Methods:** A canine cadaveric forelimb was used to model different combinations of valgus and external torsion. Valgus was induced in the limb in increments of five degrees, radiographic images were taken at each increment, and the observed radiographic valgus was measured. Various angles of torsion were then induced and the process was repeated for a range of torsional angles at 15° increments. For the second objective, the study was repeated with the forelimb rotationally repositioned to mirror the degree of the induced torsion of the deformity at each valgus and torsion iteration.

**Results:** Both zero degrees and 15° torsional iterations possessed mean artifactual valgus (AV) values between zero and five degrees for every valgus increment. With torsion of 30° and higher, mean AV values varied widely and did not fall within the zero to five degree accepted range. Rotationally re-positioning the limb in an attempt to alleviate the AV discrepancies resulted in the 30° torsional group having acceptable AV values for valgus values between zero and 20°.

**Clinical significance:** Increasing antebrachial torsion interferes with accurate radiographic measurement of frontal plane deformities. Radiographically repositioning the limb allows the accurate calculation of more valgus and torsion combinations, but still results in miscalculations of more complex deformities.

## Introduction

Within the canine appendicular skeleton, the radius and ulna are the bones most frequently affected by angular limb deformities (ALD) (1). Combined retardation of growth at the level of the distal radial and ulnar physes is the most common aetiopathogenesis of antebrachial deformities (2). Resulting angulation most frequently exists as excessive radial procurvatum, external torsion and distal radial valgus. With combination torsion-angulation deformities, neither the angulation nor the torsion can be accurately measured from standard cranial-caudal or medial-lateral orthogonal radiographic projections alone

because the radiographic appearance of the proximal and distal aspects of the bone as observed in the standard planes is altered (3). Whereas computed tomography can be successfully used to resolve such complex deformities, radiography remains the least costly and most accessible diagnostic tool for ALD pre-surgical planning (3). However, with respect to the canine radius and ulna, the degree of radiographic miscalculation utilizing standard orthogonal projections in the assessment of torsion-angulation deformities is unknown. A radiographic technique that compensates for this miscalculation has been described for the human femur and was recently adapted for the canine antebrachium, however the technique lacks scientific validation (4, 5). Therefore, the objectives of this study were to 1) quantify the effect of antebrachial torsion on the miscalculation of radial valgus measured radiographically, and 2) assess a method of radiographic positioning intended to resolve artifacts associated with antebrachial torsion to improve the measurement accuracy of the frontal plane component of the angulation. We hypothesized that with increasing torsion, accurate determination of angulation in the frontal plane would deteriorate, but that rotationally repositioning the limb would allow better estimation of the valgus.

## Materials and methods

A single forelimb from a 25 kg skeletally mature research dog that was euthanatized for reasons unrelated to the study was utilized. Radiographic images of the humerus, antebrachium and manus confirmed that there were not any apparent skeletal abnormalities. The forelimb was disarticulated at the level of the shoulder and the limb positioned in a holding device fashioned from an acrylic V-shaped trough, and a 3 mm transcondylar intramedullary pin was used to fix the humerus to the device. Radiopaque markers fashioned from the tips of 1.6 mm Kirschner wires were fluoroscopically placed at the proximal-most aspect of the lateral side of the radial head and medial coronoid process, as well as in the medial and lateral-most aspects of the distal radial articular facet, thus marking the elbow and radiocarpal joint reference lines in the frontal plane as previously described without disrupting the soft tissue around either joint (6). A two-ring, hinged circular external fixator frame with attached goniometer was applied to the distal radius, with the hinge axis, or angulation correction axis (ACA), positioned parallel to the craniocaudal plane, over the pre-determined neutral centre of rotation of angulation (CORA), and an angular motor was placed perpendicular to the ACA (Fig. 1) (7). The goniometer used was made of translucent plastic and it possessed major incremental gradations of  $10^\circ$  and minor gradations of two degrees. It was attached to the frame with cyanoacrylate glue at  $180^\circ$  of hinge extension, such that the two rings were perfectly parallel, confirmed by measuring the distance between the rings at three points. One centimetre transverse radial and ulnar osteotomies were completed on the ACA-CORA through standard cranio-medial and caudal surgical approaches respectively, and without further disruption of soft tissues. Cranio-caudal projection radiographs were taken of the limb with the elbow positioned in extension to establish baseline normal joint reference angles with respect to the radial anatomical axis based on the joint markers according to techniques previously described (Fig. 2) (6). For all radiographs taken, the radiographic beam was centred over the ACA-CORA. Baseline values for the anatomical medial proximal radial angle (aMPRA) and the anatomical lateral distal radial angle (aLDRA) were both calculated to be  $84^\circ$ .

Valgus was induced in the limb in increments of five degrees (between  $0^\circ$  and  $45^\circ$ ) utilizing the angular motor while visually confirming the angulation with the frame-mounted goniometer. Size-calibrated digital radiographs were taken in the cranio-caudal projection at each valgus increment, ensuring the elbow was positioned in extension as described

by Fasanella et al., such that the linear distance from the lateral humeral epicondyle to the lateral cortex of the olecranon was 45% of the transcondylar width  $\pm$  5% (8). The amount of observed radiographic valgus (ORV) was measured six times by a single observer utilizing digital radiography software. To achieve this, both the proximal and distal radial anatomical axes were drawn from the joint reference lines at the determined angles corresponding to the aMPRA and aLDRA as previously described (6). The point of intersection of the two axes represented the CORA, and the angular difference between the axes was measured as the CORA magnitude. Both the mean and 95% confidence intervals (CI) were calculated from the six values obtained for every valgus increment. The distal ring was then returned to zero degrees valgus and rotated such that the hinges and angular motor were each shifted one hole along the ring with respect to the bolts attaching the transfixation wires. This manipulation was equivalent to inducing 15° (the angular difference between holes) of external torsion at the osteotomy. Valgus was progressively re-induced at five degree increments and radiographed in the cranio-caudal projection. This process was repeated for torsional angles from zero to 60° at 15° increments. Each radiograph was confirmed to be 'elbow straight' by the aforementioned criteria and the CORA magnitude was measured six times as previously described. For each valgus-torsion iteration, absolute differences between the goniometric true valgus (TV) and the ORV were calculated to result in a set of artifactual valgus (AV) values from which the mean and 95% CI were calculated (Table 1). A theoretical *acceptable valgus error* of five degrees was considered to be the limit of clinically acceptable AV based on a previous study that considered residual varus or valgus  $\leq 5^\circ$  following tibial fracture reduction in human patients to be satisfactory (9). Thus, any mean AV over five degrees was considered to be a miscalculation of the valgus (or excessive AV) great enough to result in clinically unacceptable post-correctional angulation.

For the second objective, the forelimb was removed from the holding device. The methodology from the first part of the study was repeated with the forelimb rotationally positioned on the radiograph table top to mirror the degree of the induced torsion of the deformity at each valgus-torsion iteration based on the methodology of Paley and adapted for the canine antebrachium by Dismukes et al. (4, 5). The purpose of this repositioning was to compensate for radiographic artifactual miscalculation of the valgus as a result of torsion, thereby obtaining ORV values more closely matching TV values. Because the ACA-CORA was located 5 cm proximal to the radiocarpal joint, executing this positioning required the limb to be rotated prior to radiographing each valgus-torsion iteration, such that a carpal radiographic image in the cranio-caudal projection could be obtained in which all metacarpals were seen evenly, without any overlapping of their respective condyles. Because the elbow joint reference lines were torsionally affected using this view, and thus unusable to generate a proximal segment anatomical axis, a best fit line was drawn in the mid-diaphysis of the proximal radius by utilizing the mid-points of the proximal radius at levels 1/3 and 2/3 from the radial head to the osteotomy. However because the carpus was correctly positioned for a cranio-caudal projection radiograph, the distal radial radiopaque markers were used to mark the distal joint reference line, and the aLDRA was thus utilized to determine the distal radial anatomical axis. The angular differences between the proximal and distal radial anatomical axes were measured six times as previously described and recorded as the ORV. Differences between the TV and ORV were used to calculate the AV value (Fig. 3). The AV values for each valgus-torsion iteration were then averaged with 95% CI calculated (Table 2). Again, AV values over five degrees were considered to be a miscalculation of the valgus, and thus likely to result in a clinically unacceptable correction. Furthermore, for each study objective, TV values were compared with AV values for each torsional increment and Pearson's correlation coefficients were calculated and recorded using statistical software.

## Results

For the first study objective, both zero degree and 15° torsional iterations possessed mean AV values  $\leq 5^\circ$  for every valgus increment. With torsion of 30° and higher, mean AV values varied widely and were not  $\leq 5^\circ$  except for three TV iterations of the 60° torsional group (valgus 20°, 25° and 30°) (Fig. 4, Table 1). Pearson's correlation coefficients for the torsional increments of TV and AV data sets were as follows: 0° torsion:  $r=0.997$  ( $p<0.001$ ), 15° torsion:  $r=0.995$  ( $p<0.001$ ), 30° torsion:  $r=0.983$  ( $p<0.001$ ), 45° torsion:  $r=0.86$  ( $p<0.001$ ), 60° torsion:  $r=-0.47$  ( $p=0.168$ ). Rotationally re-positioning the limb in an attempt to compensate for AV discrepancies resulted in the 30° torsional group having acceptable AV values ( $\leq 5^\circ$ ) for TV values between zero to 20°, the 45° torsional group having AV values  $\leq 5^\circ$  for TV values between zero to 15°, and the 60° torsional group having AV values  $\leq 5^\circ$  for TV values between zero to 10° (Fig. 5, Table 2). Pearson's correlation coefficients for the torsional increments of TV and AV data sets were as follows: 0° torsion:  $r=0.997$  ( $p<0.001$ ), 15° torsion:  $r=0.997$  ( $p<0.001$ ), 30° torsion:  $r=0.992$  ( $p<0.001$ ), 45° torsion:  $r=0.932$  ( $p<0.001$ ), 60° torsion:  $r=0.954$  ( $p<0.001$ ).

## Discussion

The purposes of this study were firstly to document the degree of miscalculation of antebrachial angulation in the frontal plane subsequent to simultaneous torsion, and secondly to assess the validity of a radiographic positioning technique intended to compensate for the artifactual miscalculation that results from using standard orthogonal radiography in calculating valgus-torsion deformities. Although examined in the human femur, such assessment has not yet been completed for the canine radius and ulna. With respect to the study's first purpose, we demonstrated that antebrachial torsion adversely affects the accurate radiographic measurement of angulation in the frontal plane. As torsion increases, so too does the lack of correlation between TV and AV. Exceptions to this existed in the Torsion 45°-TV 20° combination and the Torsion 60°-TV 20°, 25° and 30° combinations (Fig. 4). Whereas this interrupted trend in declining measurement accuracy with increasing torsion has yet to be specifically studied, we suggest these results are a manifestation of the complex geometrical shape of the canine radius and ulna in the frontal, sagittal and axial planes. In other words, because the canine antebrachium is not a perfect cylinder, but possesses normal procurvatum in addition to the induced valgus and torsion, it stands to reason that the naturally occurring procurvatum may have an additive or diminishing effect on the appearance of valgus with certain torsional iterations if a standard cranial-caudal view of the elbow is combined with an increasingly oblique view of the carpus on the same singular radiographic projection when the joint orientation lines are used to generate the bone's axes.

Thus, the study's second purpose was to assess a radiographic method of positioning that could mitigate the discrepancy between TV and ORV with increasing torsional deformity. Results of this analysis demonstrated that direct relationships between the TV and AV for each torsional increment investigated occur with high correlation despite the lack of all valgus-torsion combinations being accurately measured. This would imply that the possibility exists to predict the true degree of angulation in the frontal plane of a limb concurrently affected with a certain degree of measurable torsion utilizing a correction factor. Radiographs provide two dimensional views of complex three-dimensional objects. As an object changes its orientation around a fixed axis in a single plane, its radiographic appearance may change in two planes. Rotational changes around multiple axes add to

the complexity of interpretation from orthogonal radiographic views. However, it is possible to use trigonometry to mathematically determine the relationship between the radiographic appearance of the object and its true orientation in three-dimensions as has been elegantly described by Cross and Newell with the radiographic appearance of the acetabular component of canine total hip replacements (10). The result of that study demonstrated how a theoretical mathematical analysis can result in the formation of a clinically useful nomogram, or a graphical analog computation device, to allow for a quick approximated calculation of the true orientation of an object from measurements provided from radiographs (10). To demonstrate the potential utility of such a device in assessing antebrachial ALD, we can consider the ability to quickly resolve the effects of torsion on the radiographic appearance of frontal plane angulation by reference to a nomogram generated from the second part of the study (Fig. 6). The nomogram was created by plotting values of the ORV in the second study against the TV values for each torsional iteration. Thus, if presented with a dog that possesses 30° of external antebrachial torsion and an ORV of 30° of valgus utilizing the technique described here, one may assume that the TV is actually closer to 45°. However, this assumes that the gross estimation of antebrachial torsion is accurate. Furthermore, the generated nomogram assumes that the canine radius has a normal degree of procurvatum and thus possesses no sagittal plane component to the deformity. It is also based on the observations of only one cadaveric limb with an artificially created angulation possessing all the aforementioned limitations. Thus, the need for mathematical analysis accounting for angulation in three planes, versus two, are truly required to generate clinically useful nomograms for the approximation of accurate calculations. Alternatively, additional diagnostic modalities are still indicated for more complex torsion-angulation deformities, including computed tomography and stereolithography (3, 5, 11, 12).

This study possessed certain limitations. A single, normal cadaveric limb was used to model an antebrachial ALD with both frontal and axial plane components *in vitro*, and thus possessed important differences from a clinical case of severe antebrachial angulation. The majority of naturally occurring antebrachial deformities in the dog would probably also possess a sagittal plane component, thus resulting in some degree of procurvatum or recurvatum. The sagittal plane component was intentionally omitted to simplify the model and allow the assessment of complex angulation combinations in a single, orthogonal plane only as a first step. Because a circular external fixator system was used to induce angulation, only torsional increments of 15° could be assessed. Thus, we can only say that the low end of the torsion range which results in frontal plane miscalculation exists somewhere between 15° and 30°, but cannot be more specific, as 15° of torsion allowed accurate estimation of valgus at each increment studied, but the 30° iteration did not. Furthermore, the method of inducing torsion in the cadaveric limb required the rotation of the distal ring, which engaged the distal radioulnar segment with two wires. But because all soft tissues were left intact over the osteotomy, there were forces resisting the torsional movement of the distal radius, ulna and associated ring when the higher levels of torsion were approached, thus resulting in some deformation of the transfixing wires. Such deformation would have resulted in under-rotation of the distal segment at higher levels of torsion, thus potentially affecting the results, although this was not quantified. This was also the main reason that the torsional component was only examined up to 60° and not beyond, despite the possibility that dogs can be affected with distal antebrachial torsion approaching 90°. Another important consideration with the study is the method by which the radial anatomical axis was determined in the second portion. Because of the rotational repositioning of the limb, the proximal radial markers could no longer be utilized to determine the anatomical axis of the proximal segment. As an alternative, this axis was generated by determining a mid-diaphyseal line based on two diametric measurements, thus still adhering to the definition of an anatomical axis as a mid-diaphyseal line.

However, it remains unknown if this necessary alteration in proximal axis determination resulted in another source of error, and if so, to what extent. Lastly, an arbitrary level of acceptable artificial miscalculation of frontal plane valgus was chosen ( $5^\circ$ ) based on work done examining the human tibia, however the level of miscalculation in the preoperative planning of ALD corrections that results in clinically unacceptable results for the canine antebrachium remains unknown (9).

In conclusion, the results of this work demonstrate that frontal plane radiographs allow for accurate determination of current frontal plane angulation for canine antebrachii possessing torsion of  $15^\circ$  or less. However,  $30^\circ$  of external torsion or greater will result in unpredictable miscalculation of valgus deformities. Radiographic repositioning of the limb to mimic the degree of torsion present broadens the range of valgus-torsion iterations that can be measured within five degrees of error, but does not allow the accurate calculation of all valgus-torsion combinations. Limbs possessing more severe combinations of frontal and axial plane deformities should undergo advanced diagnostic imaging techniques such as computed tomography or stereolithography to ensure accurate preoperative assessment and surgical planning until additional studies can further elucidate the correction factors required to make radiographic images consistently accurate for a full spectrum of antebrachial ALD.

### **Conflict of interest**

None declared.

## **References**

1. Johnson JA, Austin C, Breur GJ. Incidence of canine appendicular musculoskeletal disorders in 16 veterinary teaching hospitals from 1980 through 1989. *Vet Comp Orthop Traumatol* 1994; 7: 56–69.
2. Theyse LFH, Voorhout G, Hazewinkel HAW. Prognostic factors in treating antebrachial growth deformities with a lengthening procedure using a circular external skeletal fixation system in dogs. *Vet Surg* 2005; 34: 424–435.
3. Meola SD, Wheeler JL, Rist CL. Validation of a technique to assess radial torsion in the presence of procurvatum and valgus deformity using computed tomography: A cadaveric study. *Vet Surg* 2008; 37: 525–529.
4. Paley D. Rotation and Angulation-Rotation Deformities. In: Herzenberg JE, editor. *Principles of Deformity Correction*. 1<sup>st</sup> ed, 2<sup>nd</sup> printing. Berlin: Springer-Verlag; 2003. pg. 235–268.
5. Dismukes DI, Fox DB, Tomlinson JL, et al. Use of radiographic measures and three-dimensional computed tomographic imaging in surgical correction of an antebrachial deformity in a dog. *J Am Vet Med Assoc* 2008; 232: 68–73.
6. Fox DB, Tomlinson JL, Cook JL, et al. Principles of uniapical and biapical radial deformity correction using dome osteotomies and the center of rotation of angulation methodology in dogs. *Vet Surg* 2006; 35: 67–77.
7. Paley D. Hardware and Osteotomy considerations. In: Herzenberg JE, editor. *Principles of Deformity Correction*. 1<sup>st</sup> ed, 2<sup>nd</sup> printing. Berlin: Springer-Verlag; 2003. pg. 291–410.
8. Fasanella FJ, Tomlinson JL, Welihozkiy A, et al. Radiographic measurements of the axes and joint angles of the canine radius and ulna. *Proceedings of the 37th Veterinary Orthopedic Society Symposium*; 2010 February 20–27; Breckenridge, Colorado, USA. pg. 21.



9. Anderson LD, Hutchins WC, Wright PE, et al. Fractures of the tibia and fibula treated by cast and transfixation pins. *Clin Orthop* 1974; 105: 179–191.
10. Cross AR, Newell SM. Definition and determination of acetabular component orientation in cemented total hip arthroplasty. *Vet Surg* 2000; 29: 507–516.
11. Apelt D, Kowaleski MP, Dyce J. Comparison of computed tomographic and standard radiographic determination of tibial torsion in the dog. *Vet Surg* 2005; 34: 457–462.
12. Crosse KR, Worth AJ. Computer-assisted surgical correction of an antebrachial deformity in a dog. *Vet Comp Orthop Traumatol* 2010; 23: 354–361.

Fig 1: cadaveric forelimb mounted in the custom holding device with transcondylar pin engaged. The circular external ring fixator was placed such that the hinge axis was over the centre of the osteotomy with the articulation of a plastic goniometer mounted onto the frame.

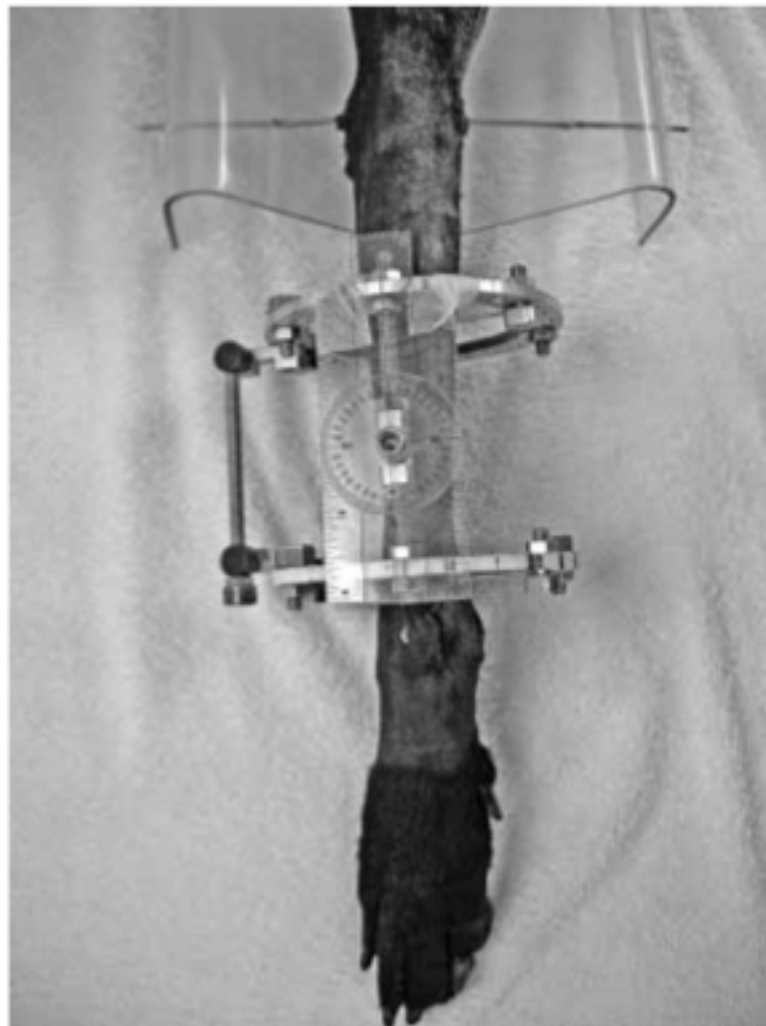
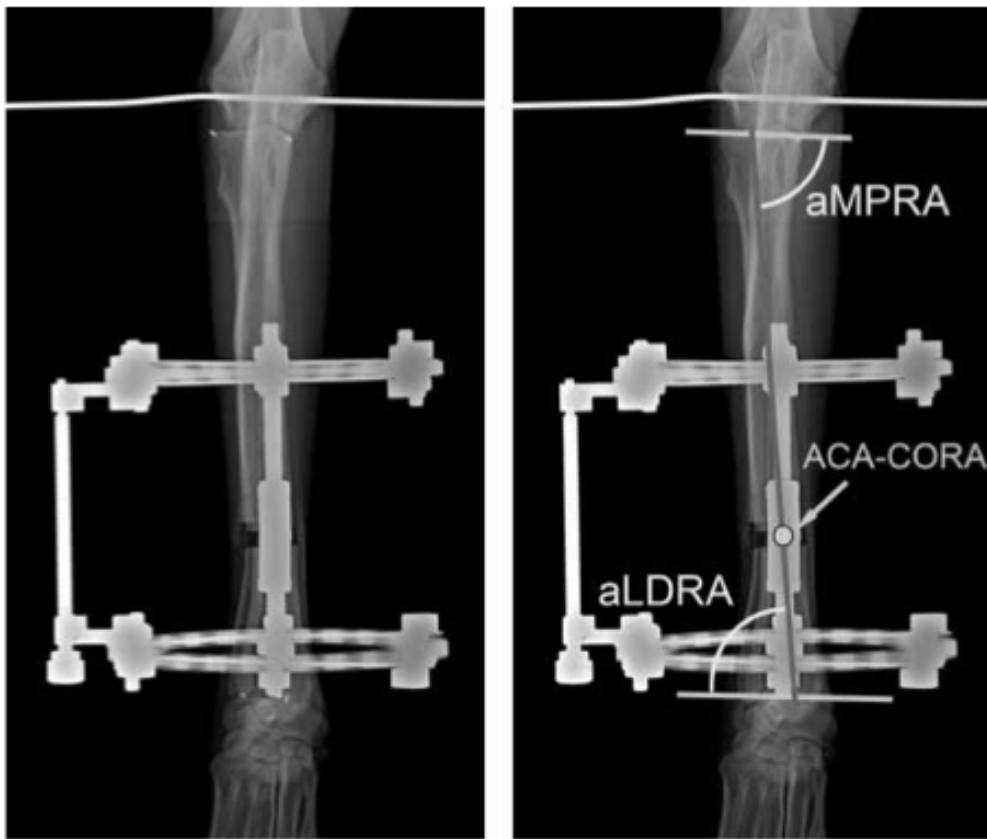


Fig 2: **A)** Frontal plane radiograph of the mounted limb with circular ring fixator in place. Radiopaque markers mark the points of the proximal and distal joint reference lines. **B)** Pre-adjustment calculation of the radial anatomic axis (grey vertical line), elbow and carpal joint reference lines (2 horizontal lines), joint orientation angles (aMPRA = anatomical medial proximal radial angle, aLDRA = anatomical lateral distal radial angle), and the ACA-CORA (angulation correction axis – centre of rotation of angulation).

Fig 3:



Representational rotationally repositioned radiograph of the limb that possessed 30° of torsion and 15° of valgus. Note that the elbow is rotationally malpositioned to allow the straight frontal plane view of the radiocarpal joint and manus. The observed radiographic valgus (ORV) in this example was measured as 16°.



Fig 4:  
 (AV) versus  
 increments of  
 The dashed  
 of clinically  
 valgus ( $5^\circ$ ).  
 this were  
 the valgus.  
 confidence  
 which are not  
 are listed in

Artificial valgus  
 true valgus (TV) for  
 increasing torsion.  
 line indicates the  
 predetermined level  
 acceptable residual  
 Values greater than  
 considered  
 miscalculations of  
 For clarity 95%  
 interval ranges,  
 shown graphically,  
 Table 1.

Fig 5: Artifactual valgus (AV) versus true valgus (TV) for increments of increasing torsion after rotationally re-positioning the limb. The dashed line indicates the predetermined level of clinically acceptable residual valgus (5°). Values greater than this were considered miscalculations of the valgus. For clarity, 95% confidence interval ranges, which are not shown graphically, are listed in Table 2.

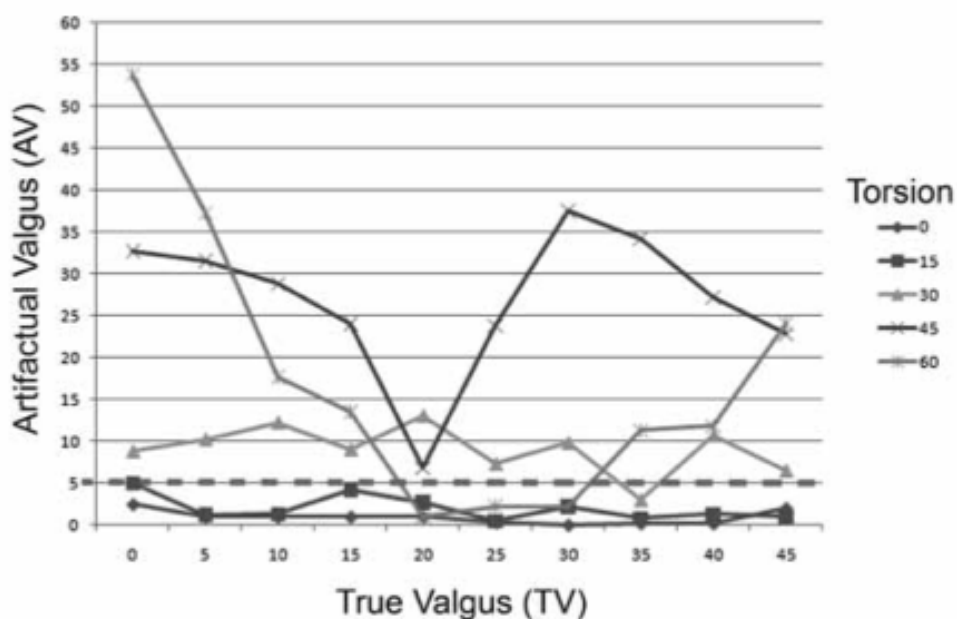
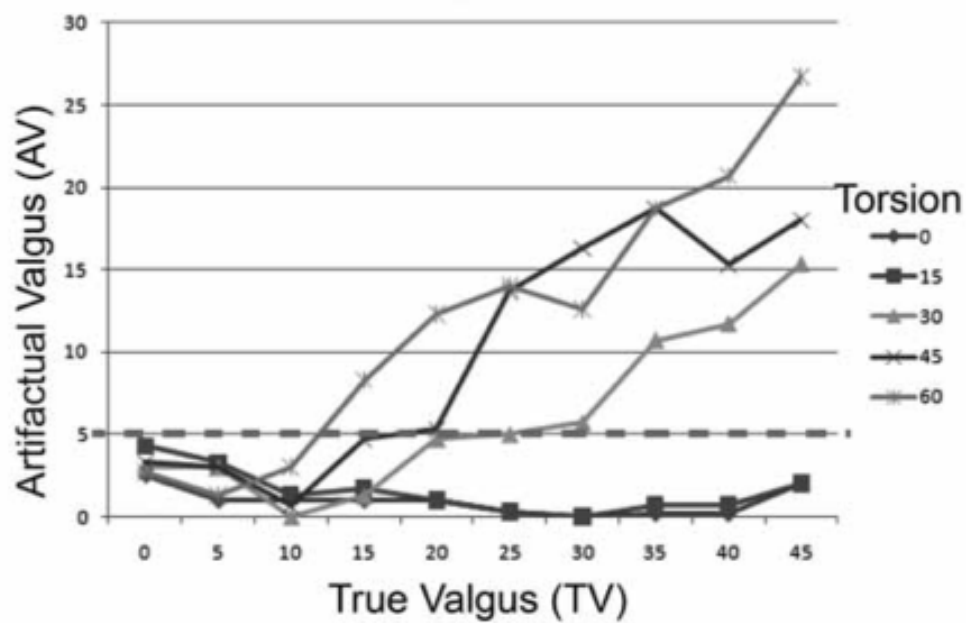
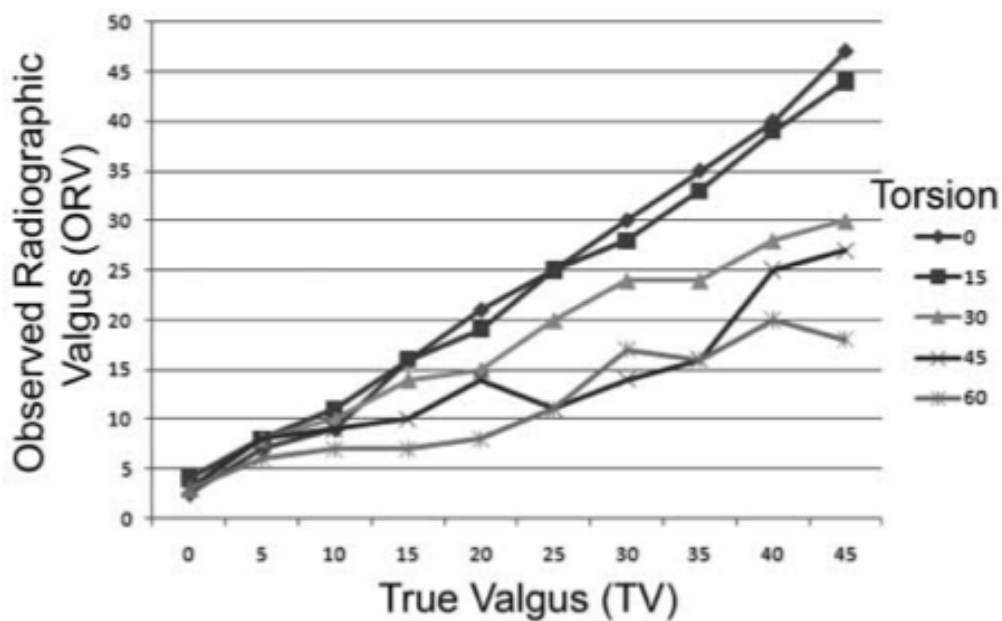


Fig 6: Nomogram generated from data depicted in Figure 5. The potential utility of this graph would allow the user to quickly approximate the true valgus (TV) from the gross



estimation of radial torsion, and observed radiographic valgus (ORV) for a radius and/or ulna affected with valgus and external torsion.

**Table 1** Artifactual valgus (AV) values calculated as the absolute difference between the true valgus (TV) and observed radiographic valgus (ORV) for the radius and ulna with created variations of valgus and external torsion. Artifactual valgus values were averaged and the 95% confidence interval (CI) was calculated for each combination. Shaded boxes signify the mean AV values that were  $\leq 5^\circ$ .



**Table 2** Artifactual valgus (AV) values calculated as the absolute difference between the true valgus (TV) and the observed radiographic valgus (ORV) for the radius and ulna with created variations of valgus and external torsion after the limb was repositioned for frontal plane radiographs. Artifactual

valgus values were averaged and the 95% confidence interval (CI) was calculated for each combination. Shaded boxes signify the mean AV values that were  $\leq 5^\circ$ .

Torsion	0°		15°		30°		45°		60°	
Valgus	Mean AV	95% CI	Mean AV	95% CI	Mean AV	95% CI	Mean AV	95% CI	Mean AV	95% CI
0°	2.5	0.8	5.0	1.6	8.8	1.4	32.7	0.8	53.7	2.19
5°	1.0	1.1	1.2	0.9	10.2	1.6	31.5	1.9	37.3	2.4
10°	1.0	1.5	1.3	1.6	12.2	1.9	28.8	2.4	17.7	2.4
15°	1.0	1.3	4.2	1.2	9.0	2.5	24.0	2.5	13.5	2.6
20°	1.0	1.0	2.7	1.1	13.0	1.0	6.8	1.1	1.0	4.5
25°	0.3	0.8	0.5	1.5	7.3	1.7	23.8	2.4	2.2	3.9
30°	0	1.9	2.2	0.8	9.8	1.4	37.5	1.9	2.2	2.0
35°	0.2	0.6	0.8	1.1	3.0	1.8	34.2	3.5	11.3	1.3
40°	0.2	1.8	1.3	1.7	10.7	1.7	27.2	2.9	11.8	6.6
45°	2.0	1.7	1.0	0.9	6.5	2.9	22.8	1.6	24.0	2.8